

1 Increased functional connectivity of thalamic subdivisions in patients with Parkinson’s  
2 disease

3  
4 Conor Owens-Walton<sup>1,\*</sup>, David Jakabek<sup>2</sup>, Brian D. Power<sup>3, 4</sup>, Mark Walterfang<sup>5,6</sup>, Dennis  
5 Velakoulis<sup>5</sup>, Danielle van Westen<sup>7, 8, ¶</sup>, Jeffrey C.L. Looi<sup>1, 5, ¶</sup>, Marnie Shaw<sup>9, ¶</sup> and Oskar  
6 Hansson<sup>10, 11, ¶</sup>

7  
8 <sup>1</sup> Research Centre for the Neurosciences of Ageing, Academic Unit of Psychiatry and  
9 Addiction Medicine, School of Clinical Medicine, Medical School, Australian National  
10 University, Canberra, Australia

11  
12 <sup>2</sup> Graduate School of Medicine, University of Wollongong, Wollongong, Australia.

13  
14 <sup>3</sup> School of Medicine, The University of Notre Dame, Fremantle, Australia

15  
16 <sup>4</sup> Clinical Research Centre, North Metropolitan Health Service – Mental Health, Perth,  
17 Australia

18  
19 <sup>5</sup> Neuropsychiatry Unit, Royal Melbourne Hospital, Melbourne Neuropsychiatry Centre,  
20 University of Melbourne & Northwestern Mental Health, Melbourne, Australia

21  
22 <sup>6</sup> Florey Institute of Neurosciences and Mental Health, University of Melbourne, Melbourne,  
23 Australia

24  
25 <sup>7</sup> Center for Medical Imaging and Physiology, Skåne University Hospital, Lund, Sweden

26  
27 <sup>8</sup> Diagnostic Radiology, Department of Clinical Sciences, Lund University, Lund, Sweden

28  
29 <sup>9</sup> College of Engineering and Computer Science, The Australian National University,  
30 Canberra, Australia

31  
32 <sup>10</sup> Memory Clinic, Skåne University Hospital, Malmö, Sweden

33  
34 <sup>11</sup> Department of Clinical Sciences, Lund University, Malmö, Sweden

35  
36  
37 \* Corresponding author: conor.owens-walton@anu.edu.au (CO-W)

38 ¶ Joint senior authors

39

## 40 **Abstract**

41 Parkinson's disease (PD) affects 2-3% of the population over the age of 65 with loss of  
42 dopaminergic neurons in the substantia nigra impacting the functioning of basal ganglia-  
43 thalamocortical circuits. The precise role played by the thalamus is unknown, despite its  
44 critical role in the functioning of the cerebral cortex, and the abnormal neuronal activity of  
45 the structure in PD. Our objective was to more clearly elucidate how functional connectivity  
46 and morphology of the thalamus are impacted in PD ( $n = 32$ ) compared to Controls ( $n = 20$ ).  
47 To investigate functional connectivity of the thalamus we subdivided the structure into two  
48 important regions-of-interest, the first with putative connections to the motor cortices and the  
49 second with putative connections to prefrontal cortices. We then investigated potential  
50 differences in the size and shape of the thalamus in PD, and how morphology and functional  
51 connectivity relate to clinical variables. Our data demonstrate that PD is associated with  
52 increases in functional connectivity between motor subdivisions of the thalamus and the  
53 supplementary motor area, and between prefrontal thalamic subdivisions and nuclei of the  
54 basal ganglia, anterior and dorsolateral prefrontal cortices, as well as the anterior and  
55 paracingulate gyri. These results suggest that PD is associated with increased functional  
56 connectivity of subdivisions of the thalamus which may be indicative alterations to basal  
57 ganglia-thalamocortical circuitry.

58

59

60

61

62

63

## 64 **Introduction**

65 Parkinson's disease (PD) is the second most common neurodegenerative disorder in the  
66 world, affecting 2-3% of the population over the age of 65 [1]. Characteristic motor  
67 symptoms of the disorder include resting tremor, rigidity and postural instability. These are  
68 accompanied by non-motor symptoms including cognitive impairment, autonomic  
69 dysfunction, disorders of sleep-wake cycle regulation, sensory disturbances and pain [2]. The  
70 neuropathological hallmark of PD is the presence of  $\alpha$ -synuclein-immunopositive Lewy  
71 bodies and neurites [3]. This neuropathology results in a degeneration of nigrostriatal  
72 dopaminergic neurons, depletion of dopamine across the striatum [4] and consequent  
73 dysfunction of basal ganglia-thalamocortical networks [5, 6].  $\alpha$ -synuclein is thought to spread  
74 from brainstem regions along the neuraxis, impacting areas of the neocortex at advanced  
75 stages of the disease [7]. Dysfunction of basal ganglia-thalamocortical circuits is thus critical  
76 as these circuits work in concert with the cortex to mediate a range of cognitive, motor and  
77 limbic functions in the brain [8].

78

79 To understand the functioning of a network, it is necessary to study the elements of the  
80 network and also their interconnections [9]. Investigating elements of brain networks can be  
81 done via studying the morphology of key neuroanatomical nuclei acting as 'hubs' within  
82 these networks [10]. Hubs are nodes within brain networks that make strong contributions to  
83 global network function [11] and the interconnections between these hubs can be investigated  
84 through the use of resting-state functional connectivity MRI methods that measure the  
85 functioning of intrinsic connectivity networks in the brain at rest [12]. Spontaneous  
86 fluctuations of the blood oxygen level-dependent (BOLD) signal that are temporally coherent  
87 indicate areas in the brain that may be functionally and anatomically related [13].

88

89 As dopamine replacement therapies provide some relief of motor symptoms in PD,  
90 significant research effort has focused on the role played by dopaminergic-depleted nuclei of  
91 the striatum [14]. However, there is now considerable evidence that the pathology underlying  
92 PD affects certain nuclei in the thalamus, and that the structure plays an important role in PD  
93 as loss of dopaminergic input to the striatum results in increased GABA-mediated inhibition  
94 of thalamocortical projections [15]. The thalamus, considered an integrative hub within  
95 functional brain networks [16], is thus an important neuroanatomical structure which we can  
96 use to investigate how basal ganglia-thalamocortical circuits are affected in PD, potentially  
97 revealing important information about the pathophysiology of the disease.

98

99 Functional connectivity (FC) studies implicating the thalamus have yielded inconsistent  
100 results with research demonstrating both increased coupling between the thalamus and  
101 sensorimotor regions in PD [17] and no significant differences in thalamic FC in PD [18].  
102 Studies have indicated that PD is associated with thalamic volumetric changes compared to  
103 control groups [19, 20], while other work presents conflicting data [21-27]. Research has  
104 demonstrated subtle morphological changes in a PD cohort compared to controls [19, 23]  
105 while other research has found no significant localized shape changes [21, 24, 26]. Although  
106 the thalamus plays a key modulatory role in the brain, there is a lack of evidence for a  
107 relationship between thalamus volumes and clinical function [21, 22, 27, 28]. Further, there is  
108 still significant information to be derived about the precise contribution of component nuclei  
109 of the structure, which are impacted differently by the pathological changes that take place in  
110 PD. We thus aimed to investigate the FC of relevant functional subdivisions within the  
111 thalamus that are crucial in mediating cognitive and motor function. We then sought to  
112 investigate possible localized structural changes to the thalamus using a morphological  
113 surface-based and volumetric analyses.

114

115 We hypothesized that there would be morphological alterations to the thalamus in PD based  
116 on the potential impact of PD neuropathology, which has been shown to display  
117 neurodegeneration post-mortem [29]. We also hypothesized that there would be a correlation  
118 between smaller overall volumes of the thalamus and poorer performance on measures of  
119 motor and cognitive function. Finally, we hypothesized that FC of important motor and  
120 prefrontal subdivisions of the thalamus would be impacted in PD due to the effect of PD  
121 disease processes on basal ganglia-thalamocortical circuits.

122

## 123 **Materials and methods**

### 124 **Participants**

125 Participants in this research were members of the Swedish BioFINDER Study  
126 ([www.biofinder.se](http://www.biofinder.se)). The study is based in Sweden and is affiliated with the Clinical Memory  
127 Research Unit and The Biomedical Centre, both at Lund University. Participants were  
128 recruited from the Memory and neurology clinics at Skåne University Hospital as well as the  
129 Memory Clinic at Ängelholm Hospital. Participants gave written informed consent and this  
130 research was performed in accordance with the World Medical Association's Declaration of  
131 Helsinki. Participants in the current study received their clinical assessments between  
132 23/05/2012 and 13/03/2014. Ethical approval was obtained through the Ethical Review Board  
133 of Lund, Sweden, and the Human Research Ethics Committee at the Australian National  
134 University, Canberra, Australia. Diagnosis of PD ( $n = 32$ ) was made by a neurologist using  
135 the National Institute of Neurological and Stroke Diagnostic criteria [30]. A healthy control  
136 group (Controls) ( $n = 20$ ) was used for comparison. Exclusion criteria for the Swedish  
137 BioFINDER study included poor knowledge of the Swedish language, developmental

138 disability, psychiatric disorder, alcohol or substance abuse, the presence of a metabolic  
139 disorder, diagnosis of probable PD dementia [31]. A preliminary investigation of functional  
140 MRI data indicated a significant difference in subject head motion during image acquisition.  
141 We therefore implemented a strict study-specific head motion exclusion criterion of >  
142 0.26mm (defined as mean relative displacement) and used advanced denoising procedures  
143 (FSL-FIX) as nuisance regression can be insufficient in removing the spurious effects of  
144 movement artifacts in MRI data [32].

145

146 All participants underwent a cognitive and neurological examination by a medical doctor  
147 with extensive experience in movement disorders. PD patients remained on medication as per  
148 their usual regime for both MRI acquisition and clinical assessment, with a levodopa  
149 equivalent dosage (LED) metric recorded for each participant. Functioning of participants  
150 was quantified with the Unified Parkinson's Disease Rating Scale Part-III test (UPDRS-III),  
151 assessing the motor signs of PD [33], the Mini Mental State Examination (MMSE), assessing  
152 cognitive mental state [34], the Timed Up and Go test (TUG), assessing mobility [35], the A  
153 Quick Test of Cognitive Speed test assessing perception and cognitive speed (AQT) [36] and  
154 the Animal Fluency test (AF), assessing verbal fluency and executive function [37].

155

## 156 **MRI acquisition**

157 Magnetic resonance imaging was performed on a 3T scanner (Trio, Siemens Magnetom,  
158 Erlangen, Germany) equipped with a 20-channel head-coil. High-resolution T1-weighted  
159 three-dimensional anatomical brain images were acquired using a magnetization-prepared  
160 rapid acquisition technique with gradient-echo sequence (repetition time = 7 ms; echo time =  
161 3 ms; flip angle = 90 degrees; voxel size = isotropic 1=mm<sup>3</sup>). Image matrix size was 356  
162 voxels in the coronal and sagittal planes and 176 voxels in the axial plane. Resting state

163 functional magnetic resonance images (rs-fMRI) (256 volumes per subject) were acquired  
164 using T2\*-weighted echo planar imaging volumes (repetition time = 1850 ms; echo time 30  
165 ms; flip angle = 90 degrees; matrix  $64 \times 64$ ; voxel size  $3 \times 3 \times 3.75 \text{ mm}^3$ ). Image matrix size  
166 was 64 voxels in the coronal and sagittal planes and 36 voxels in the axial plane. Subjects  
167 were instructed to lie still with their eyes closed, not to fall asleep and not to think of  
168 anything in particular during the scan, which lasted for approximately 8 minutes.

169

## 170 **Manual segmentation of the thalamus**

171 Manual region-of-interest tracing was performed on participant's T1 MRI data, using  
172 ANALYZE 12.0 software (Mayo Biomedical Imaging Resource, Rochester, Minnesota,  
173 USA) following a validated method [38]. The tracing for each thalamus was saved as a  
174 binary image for rs-fMRI seed-based FC and shape-based morphological analyses. A detailed  
175 explanation of the manual tracing method and associated reliability statistics is available in  
176 Supplementary Information '*Manual segmentation of the thalamus.*'

177

## 178 **Resting-state fMRI preprocessing**

179 All rs-fMRI preprocessing used FMRIB Software Library (FSL) software package tools  
180 (FMRIB Software Library, Oxford, UK; FSL version 5.0.10, RRID:SCR\_002823) [39].  
181 FMRI Expert Analysis Tool (FEAT) (version 6.00) was used for the removal of the first 6  
182 volumes, motion correction using FMRIB Motion Correction Linear Registration Tool  
183 (MCFLIRT) [40], slice-timing correction using Fourier-space timeseries phase-shifting,  
184 removal of non-brain structures using FSL's Brain Extraction Tool (BET) [41], spatial  
185 smoothing using a full-width half-maximum gaussian kernel of 5 mm, grand mean intensity  
186 normalization and high-pass temporal filtering (gaussian-weighted least-squares straight line  
187 fitting, with  $\sigma = 50.0\text{s}$ ) [42]. Registration of functional images to subjects structural

188 images used boundary-based registration [43] within the FMRIB Linear Registration Tool  
189 (FLIRT) [40, 44]. Registration of functional images to Montreal Neurological Institute (MNI)  
190 152 T1 2mm<sup>3</sup> standard space was also performed using FLIRT with 12 degrees of freedom,  
191 further refined using FNIRT nonlinear registration [45, 46] with a warp resolution of 10mm  
192 and a resampling resolution of 4mm. Denoising of head motion, scanner and cerebrospinal  
193 fluid artefacts was performed using a probabilistic Multivariate Exploratory Linear  
194 Optimized Decomposition into Independent Components (MELODIC version 3.15)  
195 independent component analysis method [47]. FSL's ICA-based Xnoiseifier (FIX version  
196 1.06) [48] was then used to classify components as either signal or noise, with noise  
197 components and also motion confounds (24 regressors) regressed from the data. For the full  
198 explanation of the denoising procedure see Supplementary Information '*Independent*  
199 *component analysis denoising.*'

200

201 The Oxford Thalamic Structural Connectivity Probability Atlas [49] within FSL's  
202 visualization GUI FSLeyes was used to parcellate bilateral thalamic manual segmentation  
203 masks into two seed regions-of-interest masks (seed-ROIs) (Fig 1), representing important  
204 functional subdivisions of the thalamus. Due to the cardinal motor symptoms in PD, our first  
205 seed-ROI incorporated voxels with the highest probability of connectivity with pre- and  
206 primary motor cortices and are intended to represent the ventral lateral posterior, ventral  
207 lateral and ventral anterior thalamic nuclei. Due to the significant cognitive dysfunction  
208 observed in PD, our second seed-ROI incorporated voxels with the highest probability of  
209 connectivity to the prefrontal cortex, intended to represent the mediodorsal and anterior  
210 thalamic nuclei [49]. For ease of reference we will refer to these seed-ROIs as the VLp/VA  
211 thalamus and MD/A thalamus, respectively. Generic VLp/VA and MD/A thalamic masks  
212 were thresholded to only include voxels that had a greater than 50% chance of inclusion, then



213 registered to subject-specific functional MRI space, and finally eroded by zeroing non-zero  
214 voxels when found in kernel, to reduce partial volume effects. A visual inspection of a subset  
215 of VLp/VA and MD/A masks was then performed to check the alignment of masks within  
216 functional data. We then extracted the mean activation of the functional data within the two  
217 seed-ROI masks at each functional timepoint for use as explanatory variables at the  
218 individual-level general linear model (GLM) stage in a mass univariate voxelwise whole-  
219 brain analysis. The average number of voxels per seed-ROI for each group and a pairwise  
220 comparison of this data is shown in Supplementary Information ‘*Atlas-based ROI*  
221 *segmentation statistics.*’

222

223

<Insert Fig 1 here>

224 **Fig 1. Positioning and likelihood-map of seed voxels for VLp/VA and MD/A thalamic**  
225 **masks.** This figure displays the voxels used in seed-ROI masks for the functional  
226 connectivity analyses, overlaid on MNI T1 0.5mm images. This image was produced by  
227 combining all of the binary masks of each participant into one unified mask, with warm  
228 (yellow - red) colors indicating the positioning of the VLp/VA voxels and cold colors (light  
229 blue - dark blue) indicating the positioning of the MD/A voxels. Darker tones are indicative  
230 of a greater proportion of voxels in that region being included in the relevant seed-ROI mask.  
231 VLp/VA, ventral lateral posterior and ventral anterior thalamic voxels; MD/A, mediodorsal  
232 and anterior thalamic voxels.

233

## 234 **Resting-state fMRI statistical analyses**

235 Two individual-level FC analyses were performed for each participant, using a GLM  
236 approach [50]. BOLD timeseries data within the VLp/VA and MD/A thalamus were  
237 correlated with activity in the rest of the brain, shifting the model with a temporal derivative  
238 to account for lags in the onset of the hemodynamic response function, removing volumes  
239 corrupted by large motion and regressing out average timeseries data from whole brain  
240 (global signal regression), white matter and ventricle masks. For the full explanation of our  
241 approach to individual-level GLM analyses, see Supplementary Information ‘*Individual-level*  
242 *GLM functional connectivity analyses.*’ Higher-level analysis of FC differences between PD

243 and Control subjects were investigated in standard space using FSL-FEAT. We chose a  
244 nonparametric permutation-based approach ( $n = 5000$ ) [51] via FSL-randomise [52] with a  
245 threshold-free cluster enhancement method controlling the family-wise error rate at  $p < 0.05$ .  
246 This approach avoids selecting arbitrary threshold values, while also potentially improving  
247 sensitivity to test signal shapes and SNR values [53]. Due to there being a significant  
248 difference in education between PD and Control groups, we included years of education as a  
249 covariate, along with age and sex.

250

## 251 **Correlation between functional connectivity and clinical data**

252 To investigate the relationship between FC and clinical variables we conducted a series of  
253 post-hoc partial correlational analyses. These focused on the average parameter estimate for  
254 VLp/VA and MD/A thalamus at the peak voxel locations derived from the between group  
255 analyses. Spherical ROIs (7mm radius) were generated around the voxel locations with the  
256 average parameter estimate extracted for each subject. Average FC for each ROI was then  
257 correlated against LED, disease duration, UPDRS-III, TUG, AQT and Animal Fluency  
258 scores.

259

## 260 **Morphology of the thalamus in PD**

### 261 **Volumetric analyses**

262 To investigate differences in volumes of the thalamus between PD and Controls we used  
263 SPSS 22.0 (IBM Corporation, Somers, New York, USA) utilizing multivariate analysis of  
264 covariance models controlling for estimated total intracranial volume (eTIV, derived from  
265 recon-all FreeSurfer processing [54]), age and sex. Effect sizes are represented by partial eta  
266 squared values ( $\eta^2$ ).

267

## 268 **Surface based shape analysis**

269 Shape analysis was performed using spherical harmonic parameterization and sampling in a  
270 three-dimensional point distribution model (SPHARM-PDM) [55] outlined in detail in  
271 Supplementary Information ‘*SPHARM-PDM detail.*’ Generally speaking, SPHARM-PDM  
272 shape analysis provides visualizations of the local surface changes to the thalamus between  
273 groups via mean difference displacement maps, mapping the magnitude of surface change  
274 (deflation or inflation) in millimeters between corresponding points on the mean surfaces of  
275 the PD subjects compared to Controls. Significant surface change was displayed at  $p < 0.05$   
276 with a correction for multiple comparisons performed using a false-discovery rate bound  $q$  of  
277 5% [56].

278

## 279 **Correlations between thalamic volumes and clinical symptoms**

280 We used hierarchical multiple regression models to assess whether thalamic volumes can  
281 predict clinical symptoms. These models incorporated two levels, the first level controlled for  
282 eTIV, age, sex and years of education (the latter when dealing with measures of cognitive  
283 function), and the second level held the independent variable of interest (volume of right or  
284 left thalamus), measuring the unique contribution of that variable in predicting each measure  
285 of clinical function. Effect sizes are represented by standardized beta values ( $\beta$ ).

286

## 287 Results

### 288 Participant characteristics

289 There were no significant differences in age, head size (eTIV) or proportions of males and  
290 females in groups, between the PD cohort and Controls. Years of education, UPDRS-III and  
291 AQT performance was significantly reduced in PD compared to Controls (Table 1).

292

293

294

295

**Table 1. Demographic and clinical characteristics of participants.**

Item	Controls	PD	<i>p</i> -value
Number of participants	20	32	-
Female/Male	10/10	18/14	0.878
Age	69.06 ± 6.86	69.36 ± 5.82	0.868
LED	-	523.36 ± 295.31	-
Disease duration	-	5.16 ± 3.62	-
eTIV (cm <sup>3</sup> )	156.81 ± 15.84	152.06 ± 17.71	0.333
Years of education	13.14 ± 3.68	9.78 ± 6.05	0.042
Relative displacement	0.13 ± 0.06	0.16 ± 0.06	0.066
H&Y	-	1.75 ± 0.55	-
UPDRS-III	2.40 ± 3.02	10.69 ± 7.06	<0.001
TUG	8.60 ± 1.54	9.68 ± 2.39	0.079
MMSE	28.8 ± 1.2	28.28 ± 1.42	0.18
AQT	57.25 ± 15.09	66.47 ± 14.78	0.035
AF	24.80 ± 6.59	23.03 ± 5.67	0.309

Data presented as mean ± standard deviation; *p*-values, one-way independent samples *t*-test, excluding male/female numbers which was analyzed via a chi-square test for independence; LED, levodopa equivalent dosage (mg); eTIV, estimated total intracranial volume; Relative displacement, mean value derived from MCFLIRT FSL motion correction; H&Y, Hoehn and Yahr Scale; UPDRS-III, Unified Parkinson's Disease Rating Scale part III; TUG, Timed Up and Go test; MMSE, Mini Mental-state Examination; AQT, A quick test of cognitive speed; AF, Animal fluency test.

296

### 297 Functional connectivity of the VLp/VA thalamus in PD

298 Analysis of the VLp/VA thalamus in PD found significant clusters of increased FC with the  
299 right supplementary motor area (BA6) and the left paracingulate gyrus (BA32). Analysis of

300 the VLp/VA thalamus also found a significant cluster of decreased FC with the left lateral  
 301 occipital cortex (BA19) (Fig 2, Table 2).

302

303 **<Insert Fig 2>**

304 **Fig 2. VLp/VA thalamus functional connectivity.** *p*-value images showing  
 305 neuroanatomical regions with significant between-group changes in functional connectivity  
 306 with the VLp/VA thalamus in PD subjects compared to Controls. Warm colors (yellow-  
 307 orange) represent areas of increased functional connectivity in PD and cool colors (light-dark  
 308 blue) represent areas of decreased functional connectivity in PD. Spacing between each slice  
 309 in the z-direction is 4.2mm beginning at  $z = -3.18$  in the top left slice (MNI T1 2mm image).  
 310 R, right; A, anterior; PCG, paracingulate gyrus; SMA, supplementary motor area; LOC,  
 311 lateral occipital cortex.

312

313

314

**Table 2. Regions showing functional connectivity differences with the VLp/VA thalamus in PD.**

FC Cluster	Peak	Brain regions	Voxels	MNI		
				x	y	z
Increased	1	R Supplementary motor area (BA6)	64	12	-2	42
	2	L Paracingulate gyrus (BA32)	11	-4	10	42
	3	R Supplementary motor area (BA6)	10	10	6	44
Decreased	4	L Lateral occipital cortex (BA19)	18	-30	-86	24
	5	L Lateral occipital cortex (BA19)	10	-26	-66	46
	6	L Lateral occipital cortex (BA19)	3	-26	-68	56

Brain regions and associated coordinates represent significant peaks within each cluster ( $p < 0.05$ ). Abbreviations: FC, functional connectivity; L, left hemisphere; R, right hemisphere; BA, Brodmann area; MNI, coordinates for location of peak voxels in Montreal Neurological Institute 152 T1 2mm space. Labelling of brain regions based on the Harvard-Oxford Cortical/Subcortical Atlases.

315

### 316 **Functional connectivity of the MD/A thalamus in PD**

317 Analysis of the MD/A thalamus in PD found significant clusters of increased FC with the left  
 318 anterior cingulate (BA24) and left putamen (Fig 3, Table 3). These clusters extended across  
 319 the following brain regions: the bilateral anterior (BA24) and paracingulate gyri (BA32), left  
 320 caudate nucleus, left putamen, left globus pallidus, bilateral dorsolateral prefrontal cortex

321 (BA9) and bilateral anterior prefrontal cortex (BA8). Analysis of the VLp/VA thalamus also  
322 found a significant cluster of decreased FC with the left lateral occipital cortex (BA19).

323

324

<Insert Fig 3>

325 **Fig 3. MD/A thalamus functional connectivity.** *p*-value images showing neuroanatomical  
326 regions with significant between-group changes in functional connectivity of the MD/A  
327 thalamus in PD subjects compared to Controls. Warm colors (yellow-orange) represent areas  
328 of increased functional connectivity in PD. Spacing between each slice in the z-direction is  
329 4mm beginning at  $z = -2.3$  in the top left slice (MNI T1 2mm image). R, right; A, anterior;  
330 Put, putamen; GP, globus pallidus; CN, caudate nucleus; PCG, paracingulate gyrus; ACC,  
331 anterior cingulate cortex; DLPFC, dorsolateral prefrontal cortex; APFC, anterior prefrontal  
332 cortex.

333

334

335

**Table 3. Regions showing functional connectivity differences with the MD/A thalamus in PD.**

FC Cluster	Peak	Brain regions	Voxels	MNI		
				x	y	z
Increased	7	L anterior cingulate (BA24)	4319	-8	18	22
	8	L putamen (BA49)	268	-20	10	-4
Decreased	9	L lateral occipital cortex (BA19)	10	-18	-78	52

Brain regions and associated coordinates represent significant peaks within each cluster ( $p < 0.05$ ). Abbreviations: FC, functional connectivity; L, left hemisphere; R, right hemisphere; BA, Brodmann area; MNI, coordinates for location of peak voxels in Montreal Neurological Institute 152 T1 2mm space; Labelling of brain regions are based on the Harvard-Oxford Cortical/Subcortical Atlases.

336

### 337 **Correlation between functional connectivity and clinical data**

338 In PD patients we observed a positive correlation between LED and mean FC of the right  
339 supplementary motor area (peak 3;  $r = 0.46$ ,  $p = 0.01$ ) and a negative correlation with the left  
340 lateral occipital cortex (peak 4;  $r = -0.41$ ,  $p = 0.04$ ). We also observed a positive correlation  
341 between disease duration and mean FC of the right supplementary motor area (peak 1;  $r =$   
342  $0.41$ ,  $p = 0.03$ ; peak 3;  $r = 0.57$ ,  $p = 0.01$ ). We also observed a positive correlation between  
343 TUG scores and mean FC of the left paracingulate gyrus (peak 2;  $r = 0.43$ ,  $p = 0.02$ ) and

344 lateral occipital cortex (peak 6;  $r = 0.43$ ,  $p = 0.02$ ; peak 9;  $r = 0.37$ ,  $p = 0.047$ ). None of these  
345 results survived correction for multiple comparisons (*Supplementary Information Table S1*).

346

## 347 **Morphology of the thalamus in PD**

### 348 **Volumetric analyses**

349 Comparisons of thalamic volumes found no difference between the PD group and Controls  
350 (Table 4).

351

352

353

354

**Table 4: Estimated mean volumes of right and left thalamus and pairwise comparison.**

Structure	Control	PD	Mean difference	<i>p</i> -value
Right thalamus volume (mm <sup>3</sup> )	5774.13	5927.45	-153.32	0.25
Left thalamus volume (mm <sup>3</sup> )	5594.47	5749.24	-154.78	0.18

Estimated volumes of the right and left thalamus after adjusting for age, eTIV and sex. *p*-value presented has been adjusted for family-wise error rate using a Bonferroni correction.

355

### 356 **Surface based shape analysis**

357 Shape analysis found no localized areas of shape change to the surface of the right or left  
358 thalamus in the PD group compared to Controls, after correcting for false-discovery rate (Fig  
359 4).

360

361

**<Insert Fig 4>**

362 **Fig 4. Shape analysis of thalamus in PD compared to Controls.** Displayed are superior  
363 and inferior views of bilateral thalami overlaid on axial MNI T1 0.5mm images. Warmer  
364 colors indicate regions of greater inflation in the PD group compared to Controls using point-  
365 wise significance tests ( $p < 0.05$ , uncorrected). No regions were significant after false-  
366 discovery rate correction.

367

## 368 **Correlations between thalamic volumes and clinical symptoms in**

### 369 **PD**

370 We found no significant relationships between volumes of the right or left thalamus and  
371 clinical function in the PD or Control groups (*Supplementary Information Table S2*).

372

### 373 **Discussion**

374 The results of this study demonstrate that PD patients on medication have increased FC  
375 within motor, dorsolateral and anterior cingulate basal ganglia-thalamocortical circuits. Our  
376 data support the findings of a recent meta-analysis showing that PD patients have increased  
377 FC of basal ganglia-thalamocortical circuitry [57], and extend these findings by showing how  
378 important functional subterritories of the thalamus are impacted in PD. These changes in FC  
379 were found despite any evidence of morphological alterations to the thalamus.

380

381 Our findings of increased FC between the VLp/VA thalamus and the supplementary motor  
382 area may be indicative of changes within one segment of the classic ‘motor’ basal ganglia-  
383 thalamocortical circuit [5]. In this model, the motor circuit originates at the supplementary  
384 motor area, receiving input from the primary and the premotor cortices. These areas connect  
385 with the nuclei of the basal ganglia, which project back to the ventral anterior and ventral  
386 lateral nuclei of the thalamus, closing the loop by reconnecting with the site of origin in  
387 motor cortical areas [5]. Increased FC between the putamen and the supplementary motor  
388 area has been demonstrated previously [58] while other research using graph theoretical  
389 analyses has demonstrated increased functional connectivity within the sensorimotor network  
390 in PD [59]. Evidence suggests that increased FC of sensorimotor networks is likely related to



391 dopaminergic medication usage [60] potentially facilitating increases in FC, which is a  
392 mechanism that will be discussed momentarily.

393

394 Our research also demonstrates significant and far more widespread increases in FC in PD  
395 between the MD/A thalamus and the anterior and dorsolateral prefrontal cortices, potentially  
396 indicating a disease related change to the ‘dorsolateral prefrontal’ basal ganglia-  
397 thalamocortical circuit [5]. This circuit originates in Brodmann areas 9 and 10 on the lateral  
398 surface of the anterior frontal lobe, and after traversing the basal ganglia, connects directly  
399 with our intended seed-ROIs at the anterior and mediodorsal nuclei of the thalamus. From  
400 there, the circuit projects back to the anterior and dorsolateral prefrontal cortices to form a  
401 closed loop [5]. Our findings of increased FC between the MD/A thalamus and the  
402 dorsolateral prefrontal cortex may represent functional compensatory mechanisms due to the  
403 significant cognitive dysfunction common in PD. The dorsolateral prefrontal cortex helps to  
404 execute tasks that contribute to cognitive functioning, including working memory, decision-  
405 making and action control, achieved through a top-down modulation of behavior in concert  
406 with diverse cortical and subcortical structures [61]. Research has shown that FC is  
407 significantly increased *across* the prefrontal cortex in PD subjects on medication, as the brain  
408 potentially recruits new anatomical areas to aid in the performance of cognitive tasks. It is  
409 argued that changes in FC may indicate a functional compensation to help restore cognitive  
410 processes in PD [61]. Interestingly, we also found significant increases in FC between the  
411 MD/A thalamus and the anterior cingulate cortex in PD subjects, indicating a disease related  
412 change to the ‘anterior cingulate’ basal ganglia-thalamocortical circuit. In this circuit, the  
413 anterior cingulate cortex links with the ventral basal ganglia structures, outputs to the ventral  
414 anterior nuclei of the thalamus, and links back with the anterior cingulate cortex [5]. Our  
415 findings of increased FC with the anterior as well as paracingulate gyri fit with the concept of

416 increased FC due to compensatory mechanisms, as this region of the brain interacts with the  
417 lateral prefrontal cortex to mediate performance in tasks linked to cognitive processes [62].  
418 Research has shown that a common response to neurological disruption is the *hyper-*  
419 connectivity of brain circuits, which may reflect a protective mechanism in the brain to  
420 maintain normal functioning [63]. Such a mechanism has been proposed in PD previously  
421 [64, 65], as well as in mild cognitive impairment and Alzheimer disease [66, 67], and taken  
422 together, our results provide support for this model.

423

424 There are nonetheless inconsistencies with similar FC research that require consideration.  
425 Our data contrast with work demonstrating no significant FC changes between the thalamus  
426 and widescale brain networks in subjects on medication [18]. A possible explanation for this  
427 inconsistency may relate to how FC changes across different disease stages. When compared  
428 to the current work, the study in question focused on PD subjects with both a longer disease  
429 duration as well as a higher average Hoehn and Yahr stage [18]. This is important because  
430 research has shown that FC in PD may undergo periods of both *hyper-connectivity* and *hypo-*  
431 connectivity as the disease progresses [64]. Potential FC changes across the course of PD  
432 thus make difficult to compare studies with subjects at different disease stages.

433

434 Our data also indicate that PD is associated with increases in FC between the MD/A thalamus  
435 and the left dorsal caudate nuclei, anterior putamen and globus pallidus. Strong evidence  
436 suggests that the output of the basal ganglia, mainly the globus pallidus interna, is  
437 hyperactive in PD [68] and our results of increased FC with this area suggest that increased  
438 activity may be accompanied by increased FC. Increased FC between the caudate nuclei and  
439 the thalamus has been shown in a PD cohort on medication [69], however two studies have  
440 demonstrated conflicting results [17, 70]. A crucial difference separating these studies relates

441 to patient inclusion. One of these studies focused on early PD patients with a mean disease  
442 duration of 1.7 years [17], which differs markedly from the current study where the average  
443 disease duration is 5.16 years. The present study also excluded PD subjects with dementia,  
444 fundamentally distinguishing it from our previous work [70]. This is crucial as PD dementia  
445 is associated with decreases in FC compared to subjects without the diagnosis [71]. Our  
446 findings of increased FC between the MD/A thalamus and the anterior putamen are supported  
447 by similar research in this field [65]. This research demonstrated that increased inter-regional  
448 coupling of the anterior putamen, the region anterior to the anterior commissure, follow the  
449 specific spatial pattern of dopamine depletion in PD [4]. This research suggests that PD  
450 patients may undergo a shift in cortico-striatal connections from the neuro-chemically more  
451 affected posterior putamen toward the relatively spared anterior putamen. Our results support  
452 this finding, suggesting that the anterior putamen may undergo increased FC with the MD/A  
453 thalamus, further supporting the model that the pathophysiology of PD may involve  
454 compensatory alterations in the FC of key nuclei within basal ganglia-thalamocortical  
455 circuits.

456

457 While conceiving of FC changes in terms of segregated basal ganglia-thalamocortical circuits  
458 is attractive, this inference is theoretical. It is therefore helpful to consider the results of other  
459 imaging techniques to substantiate our findings. Graph-based eigenvector centrality mapping  
460 research (which informs on the number and quality of node connections within networks) has  
461 shown that this metric is increased in the thalamus in PD [72]. Interestingly, we also found a  
462 significant (though small) cluster of reduced FC of both the VLp/VA and MD/A thalamus  
463 with the lateral occipital cortex in PD patients, supporting previous work which found  
464 reductions in FC between nuclei of the extended basal-ganglia (including the thalamus) and  
465 this area of the brain [72]. The findings from  $^{18}\text{F}$ -flurodeoxyglucose PET imaging has

466 indicated that PD is associated with increased pallidothalamic activity [73], which supports  
467 our findings. However, this research also demonstrated that regions of the dorsolateral  
468 prefrontal cortex and the supplementary and premotor areas show reductions in metabolic  
469 activity in PD, contrasting with our results [73].

470

471 We found no significant correlation between FC of our seed-ROI in the thalamus and  
472 measures of clinical function, disease duration or antiparkinsonian medication use. This  
473 supports previous meta-analytic research which indicates that FC within a basal-ganglia  
474 networks does not correlate with clinical indices of disease severity [74], arguing instead that  
475 altered FC reflects a constitutional alteration of the networks under consideration. Our results  
476 are also bolstered by meta-analytic findings which indicate that increased FC of the thalamus  
477 were unaffected by medication status [57].

478

479 The morphological data from our study are consistent with previous reports indicating that  
480 PD is not associated with atrophy of the thalamus [21, 23-28]. We also found no significant  
481 localized surface shape changes in the PD group, supporting a number of studies [21, 24, 25].  
482 After investigating between-group morphological differences we investigated potential  
483 relationships between volumes of the thalamus and measures of clinical function. These  
484 analyses revealed no significant findings, supporting previous research [21, 27, 28]. These  
485 results make intuitive sense, as we found no significant volumetric or localized shape  
486 changes in the PD cohort, suggesting there was no discernable relationship between atrophy  
487 of the thalamus and the PD disease process.

488

## 489 **Strengths and Limitations**

490 Possible limitations of the current work warrant further attention. The first is our small  
491 sample size. While this is an important factor that negatively impacts the power of our study,  
492 our sample size was the result of choosing a highly stringent head motion exclusion criteria,  
493 which we believe is a strength of our work. A second possible limitation is the use of atlas-  
494 based seed-ROI segmentation, defined by the structural connectivity of thalamic nuclei [49].  
495 Future work may benefit from a data-driven parcellation scheme as it may better capture  
496 functional boundaries of seed-ROIs. Despite these considerations we believe our data make  
497 important statements about the role of the thalamus within basal ganglia-thalamocortical  
498 circuits in PD.

499

## 500 **Conclusions**

501 We found increases in functional connectivity between the VLp/VA thalamus and the  
502 supplementary motor area and paracingulate gyrus, and also between the MD/A thalamus and  
503 basal ganglia nuclei, anterior and paracingulate cingulate gyri, anterior and also dorsolateral  
504 prefrontal cortical regions. Significant increases in functional connectivity were found despite  
505 any observable volumetric or localized shape alterations to the thalamus. The results of this  
506 study indicate that functional connectivity changes occur in PD, which likely result from  
507 disease-related system level dysfunction of the thalamus as a crucial network hub within  
508 basal ganglia-thalamocortical circuits.

509

## 510 **Acknowledgements**

511 The authors are indebted to all patients and control subjects who participated in this study.  
512 This project is an initiative of the Swedish BioFINDER Study, of whom DvW and OH are

513 steering committee members, and also the AUSSIE network coordinated by JCLL at the  
514 Australian National University Medical School, who self-funds related expenses.

515

#### 516 **Financial disclosure statement**

517 CO-W would like to acknowledge The Australian National University for their funding  
518 support via the University Research Scholarship. Work in DvW and OH's laboratory was  
519 supported by the European Research Council, the Swedish Research Council, the Strategic  
520 Research Area MultiPark (Multidisciplinary Research in Parkinson's disease) at Lund  
521 University, the Swedish Brain Foundation, the Parkinson Foundation of Sweden, the Skåne  
522 University Hospital Foundation and the Swedish federal government under the ALF  
523 agreement. Funding sources had no role in the conduct of this study, its analysis,  
524 interpretation of the data or in the preparation, review or approval of the manuscript.

525

526

#### References

527

- 528 1. Poewe W, Seppi K, Tanner CM, Halliday GM, Brundin P, Volkman J, et al.  
529 Parkinson disease. *Nature Reviews Disease Primers*. 2017;3:17013.
- 530 2. Schapira AHV, Chaudhuri KR, Jenner P. Non-motor features of Parkinson disease.  
531 *Nat Rev Neurosci*. 2017;18(7):435-50.
- 532 3. Dickson DW, Braak H, Duda JE, Duyckaerts C, Gasser T, Halliday GM, et al.  
533 Neuropathological assessment of Parkinson's disease: refining the diagnostic criteria.  
534 *The Lancet Neurology*. 2009;8(12):1150-7.
- 535 4. Kish SJ, Shannak K, Hornykiewicz O. Uneven pattern of dopamine loss in the  
536 striatum of patients with idiopathic Parkinson's disease. Pathophysiologic and clinical  
537 implications. *New England Journal of Medicine*. 1988;318(14):876-80.
- 538 5. Alexander GE, DeLong MR, Strick PL. Parallel organization of functionally  
539 segregated circuits linking basal ganglia and cortex. *Annual review of neuroscience*.  
540 1986;9(1):357-81.
- 541 6. DeLong M, Wichmann T. Update on models of basal ganglia function and  
542 dysfunction. *Parkinsonism & Related Disorders*. 2009;15:S237-S40.
- 543 7. Braak H, Del Tredici K, Rüb U, de Vos RA, Jansen Steur EN, Braak E. Staging of  
544 brain pathology related to sporadic Parkinson's disease. *Neurobiology of Aging*.  
545 2003;24(2):197-211.
- 546 8. Haber SN. The primate basal ganglia: parallel and integrative networks. *Journal of*  
547 *chemical neuroanatomy*. 2003;26(4):317-30.

- 548 9. Sporns O, Tononi G, Kötter R. The Human Connectome: A Structural Description of  
549 the Human Brain. *PLoS Computational Biology*. 2005;1(4).
- 550 10. Sporns O, Honey CJ, Kötter R. Identification and classification of hubs in brain  
551 networks. *PloS one*. 2007;2(10):e1049.
- 552 11. van den Heuvel MP, Sporns O. Network hubs in the human brain. *Trends in cognitive*  
553 *sciences*. 2013;17(12):683-96.
- 554 12. Biswal B, Yetkin FZ, Haughton VM, Hyde JS. Functional connectivity in the motor  
555 cortex of resting human brain using echo-planar MRI. *Magn Reson Med*.  
556 1995;34(4):537-41.
- 557 13. Fox MD, Raichle ME. Spontaneous fluctuations in brain activity observed with  
558 functional magnetic resonance imaging. *Nat Rev Neurosci*. 2007;8(9):700-11.
- 559 14. Caligiore D, Helmich RC, Hallett M, Moustafa AA, Timmermann L, Toni I, et al.  
560 Parkinson's disease as a system-level disorder. *npj Parkinson's Disease*.  
561 2016;2:16025.
- 562 15. Obeso JA, Rodríguez - Oroz MC, Benitez - Temino B, Blesa FJ, Guridi J, Marin C,  
563 et al. Functional organization of the basal ganglia: therapeutic implications for  
564 Parkinson's disease. *Movement Disorders*. 2008;23(S3):S548-S59.
- 565 16. Hwang K, Bertolero MA, Liu WB, D'esposito M. The human thalamus is an  
566 integrative hub for functional brain networks. *Journal of Neuroscience*.  
567 2017;37(23):5594-607.
- 568 17. Agosta F, Caso F, Stankovic I, Inuggi A, Petrovic I, Svetel M, et al. Cortico-striatal-  
569 thalamic network functional connectivity in hemiparkinsonism. *Neurobiology of*  
570 *Aging*. 2014;35(11):2592-602.
- 571 18. Bell PT, Gilat M, O'Callaghan C, Copland DA, Frank MJ, Lewis SJG, et al.  
572 Dopaminergic basis for impairments in functional connectivity across subdivisions of  
573 the striatum in Parkinson's disease. *Human Brain Mapping*. 2015;36(4):1278-91.
- 574 19. Garg A, Appel-Cresswell S, Popuri K, McKeown MJ, Beg MF. Morphological  
575 alterations in the caudate, putamen, pallidum, and thalamus in Parkinson's disease.  
576 *Frontiers in Neuroscience*. 2015;9.
- 577 20. Lee S, Kim S, Tae W, Lee S, Choi J, Koh S, et al. Regional volume analysis of the  
578 Parkinson disease brain in early disease stage: gray matter, white matter, striatum, and  
579 thalamus. *American Journal of Neuroradiology*. 2011;32(4):682-7.
- 580 21. Lee HM, Kwon K-Y, Kim M-J, Jang J-W, Suh S-i, Koh S-B, et al. Subcortical grey  
581 matter changes in untreated, early stage Parkinson's disease without dementia.  
582 *Parkinsonism & related disorders*. 2014;20(6):622-6.
- 583 22. Mak E, Su L, Williams GB, Firbank MJ, Lawson RA, Yarnall AJ, et al. Baseline and  
584 longitudinal grey matter changes in newly diagnosed Parkinson's disease: ICICLE-  
585 PD study. *Brain*. 2015;138(10):2974-86.
- 586 23. McKeown MJ, Uthama A, Abugharbieh R, Palmer S, Lewis M, Huang X. Shape (but  
587 not volume) changes in the thalami in Parkinson disease. *BMC neurology*.  
588 2008;8(1):8.
- 589 24. Menke RA, Szewczyk - Krolkowski K, Jbabdi S, Jenkinson M, Talbot K, Mackay  
590 CE, et al. Comprehensive morphometry of subcortical grey matter structures in  
591 early - stage Parkinson's disease. *Human brain mapping*. 2014;35(4):1681-90.
- 592 25. Messina D, Cerasa A, Condino F, Arabia G, Novellino F, Nicoletti G, et al. Patterns  
593 of brain atrophy in Parkinson's disease, progressive supranuclear palsy and multiple  
594 system atrophy. *Parkinsonism & related disorders*. 2011;17(3):172-6.
- 595 26. Nemmi F, Sabatini U, Rascol O, Peran P. Parkinson's disease and local atrophy in  
596 subcortical nuclei: insight from shape analysis. *Neurobiology of Aging*.  
597 2015;36(1):424-33.

- 598 27. Tinaz S, Courtney MG, Stern CE. Focal cortical and subcortical atrophy in early  
599 Parkinson's disease. *Movement Disorders*. 2011;26(3):436-41.
- 600 28. Mak E, Bergsland N, Dwyer MG, Zivadinov R, Kandiah N. Subcortical atrophy is  
601 associated with cognitive impairment in mild Parkinson disease: a combined  
602 investigation of volumetric changes, cortical thickness, and vertex-based shape  
603 analysis. *American Journal of Neuroradiology*. 2014;35(12):2257-64.
- 604 29. Halliday GM. Thalamic changes in Parkinson's disease. *Parkinsonism & Related  
605 Disorders*. 2009;15, Supplement 3:S152-S5.
- 606 30. Gelb DJ, Oliver E, Gilman S. Diagnostic criteria for Parkinson disease. *Archives of  
607 neurology*. 1999;56(1):33-9.
- 608 31. Emre M, Aarsland D, Brown R, Burn DJ, Duyckaerts C, Mizuno Y, et al. Clinical  
609 diagnostic criteria for dementia associated with Parkinson's disease. *Movement  
610 Disorders*. 2007;22(12):1689-707; quiz 837.
- 611 32. Power JD, Barnes KA, Snyder AZ, Schlaggar BL, Petersen SE. Spurious but  
612 systematic correlations in functional connectivity MRI networks arise from subject  
613 motion. *Neuroimage*. 2012;59(3):2142-54.
- 614 33. Fahn S, Elton R, editors. Members of the UPDRS development committee: The  
615 unified Parkinson disease rating scale. Florham Park, NJ.: Macmillan Health Care  
616 Information; 1987.
- 617 34. Folstein MF, Folstein SE, McHugh PR. "Mini-mental state": a practical method for  
618 grading the cognitive state of patients for the clinician. *Journal of psychiatric  
619 research*. 1975;12(3):189-98.
- 620 35. Podsiadlo D, Richardson S. The timed "Up & Go": a test of basic functional mobility  
621 for frail elderly persons. *Journal of the American Geriatrics Society*. 1991;39(2):142-  
622 8.
- 623 36. Palmqvist S, Minthon L, Wattmo C, Londos E, Hansson O. A Quick Test of cognitive  
624 speed is sensitive in detecting early treatment response in Alzheimer's disease.  
625 *Alzheimer's research & therapy*. 2010;2(5):29.
- 626 37. Tombaugh TN, Kozak J, Rees L. Normative data stratified by age and education for  
627 two measures of verbal fluency: FAS and animal naming. *Archives of Clinical  
628 Neuropsychology*. 1999;14(2):167-77.
- 629 38. Power BD, Wilkes FA, Hunter-Dickson M, van Westen D, Santillo AF, Walterfang  
630 M, et al. Validation of a protocol for manual segmentation of the thalamus on  
631 magnetic resonance imaging scans. *Psychiatry Research: Neuroimaging*.  
632 2015;232(1):98-105.
- 633 39. Jenkinson M, Beckmann CF, Behrens TEJ, Woolrich MW, Smith SM. FSL.  
634 *Neuroimage*. 2012;62(2):782-90.
- 635 40. Jenkinson M, Bannister P, Brady M, Smith S. Improved optimization for the robust  
636 and accurate linear registration and motion correction of brain images. *Neuroimage*.  
637 2002;17(2):825-41.
- 638 41. Smith SM. Fast robust automated brain extraction. *Human brain mapping*.  
639 2002;17(3):143-55.
- 640 42. Woolrich MW, Ripley BD, Brady M, Smith SM. Temporal autocorrelation in  
641 univariate linear modeling of fMRI data. *Neuroimage*. 2001;14(6):1370-86.
- 642 43. Greve DN, Fischl B. Accurate and robust brain image alignment using boundary-  
643 based registration. *Neuroimage*. 2009;48(1):63-72.
- 644 44. Jenkinson M, Smith S. A global optimisation method for robust affine registration of  
645 brain images. *Medical image analysis*. 2001;5(2):143-56.
- 646 45. Andersson JLR, Jenkinson M, Smith SM. Non-linear optimisation. FMRIB technical  
647 report TR07JA1. 2007.



- 648 46. Andersson JLR, Jenkinson M, Smith SM. Non-linear optimisation, aka spatial  
649 normalisation. FMRIB technical report TR07JA2. 2007.
- 650 47. Beckmann CF, Smith SM. Probabilistic independent component analysis for  
651 functional magnetic resonance imaging. *IEEE transactions on medical imaging*.  
652 2004;23(2):137-52.
- 653 48. Salimi-Khorshidi G, Douaud G, Beckmann CF, Glasser MF, Griffanti L, Smith SM.  
654 Automatic denoising of functional MRI data: combining independent component  
655 analysis and hierarchical fusion of classifiers. *Neuroimage*. 2014;90:449-68.
- 656 49. Behrens TE, Johansen-Berg H, Woolrich MW, Smith SM, Wheeler-Kingshott CA,  
657 Boulby PA, et al. Non-invasive mapping of connections between human thalamus and  
658 cortex using diffusion imaging. *Nature Neuroscience*. 2003;6(7):750-7.
- 659 50. Woolrich MW, Behrens TEJ, Beckmann CF, Jenkinson M, Smith SM. Multilevel  
660 linear modelling for fMRI group analysis using Bayesian inference. *Neuroimage*.  
661 2004;21(4):1732-47.
- 662 51. Nichols TE, Holmes AP. Nonparametric permutation tests for functional  
663 neuroimaging: a primer with examples. *Hum Brain Mapp*. 2002;15(1):1-25.
- 664 52. Winkler AM, Ridgway GR, Webster MA, Smith SM, Nichols TE. Permutation  
665 inference for the general linear model. *Neuroimage*. 2014;92:381-97.
- 666 53. Smith SM, Nichols TE. Threshold-free cluster enhancement: addressing problems of  
667 smoothing, threshold dependence and localisation in cluster inference. *Neuroimage*.  
668 2009;44(1):83-98.
- 669 54. Fischl B. FreeSurfer. *Neuroimage*. 2012;62(2):774-81.
- 670 55. Styner M, Oguz I, Xu S, Brechbuhler C, Pantazis D, Levitt JJ, et al. Framework for  
671 the Statistical Shape Analysis of Brain Structures using SPHARM-PDM. *The insight*  
672 *journal*. 2006(1071):242-50.
- 673 56. Genovese CR, Lazar NA, Nichols T. Thresholding of statistical maps in functional  
674 neuroimaging using the false discovery rate. *Neuroimage*. 2002;15(4):870-8.
- 675 57. Ji G-J, Hu P, Liu T-T, Li Y, Chen X, Zhu C, et al. Functional Connectivity of the  
676 Corticobasal Ganglia–Thalamocortical Network in Parkinson Disease: A Systematic  
677 Review and Meta-Analysis with Cross-Validation. *Radiology*. 2018;287(3):172183.
- 678 58. Yu R, Liu B, Wang L, Chen J, Liu X. Enhanced Functional Connectivity between  
679 Putamen and Supplementary Motor Area in Parkinson’s Disease Patients. *PLOS*  
680 *ONE*. 2013;8(3):e59717.
- 681 59. Göttlich M, Münte TF, Heldmann M, Kasten M, Hagenah J, Krämer UM. Altered  
682 Resting State Brain Networks in Parkinson’s Disease. *PLOS ONE*.  
683 2013;8(10):e77336.
- 684 60. Esposito F, Tessitore A, Giordano A, De Micco R, Paccone A, Conforti R, et al.  
685 Rhythm-specific modulation of the sensorimotor network in drug-naïve patients with  
686 Parkinson’s disease by levodopa. *Brain*. 2013;136(3):710-25.
- 687 61. Caspers J, Mathys C, Hoffstaedter F, Südmeyer M, Cieslik EC, Rubbert C, et al.  
688 Differential Functional Connectivity Alterations of Two Subdivisions within the  
689 Right dlPFC in Parkinson’s Disease. *Frontiers in Human Neuroscience*. 2017;11:288.
- 690 62. Fornito A, Yucel M, Wood S, Stuart GW, Buchanan JA, Proffitt T, et al. Individual  
691 differences in anterior cingulate/paracingulate morphology are related to executive  
692 functions in healthy males. *Cerebral cortex (New York, NY : 1991)*. 2004;14(4):424-  
693 31.
- 694 63. Hillary FG, Roman CA, Venkatesan U, Rajtmajer SM, Bajo R, Castellanos ND.  
695 Hyperconnectivity is a fundamental response to neurological disruption.  
696 *Neuropsychology*. 2015;29(1):59-75.

- 697 64. Gorges M, Muller HP, Lule D, Pinkhardt EH, Ludolph AC, Kassubek J. To rise and  
698 to fall: functional connectivity in cognitively normal and cognitively impaired  
699 patients with Parkinson's disease. *Neurobiology of Aging*. 2015;36(4):1727-35.  
700 65. Helmich RC, Derikx LC, Bakker M, Scheeringa R, Bloem BR, Toni I. Spatial  
701 remapping of cortico-striatal connectivity in Parkinson's disease. *Cerebral cortex*.  
702 2010;20(5):1175-86.  
703 66. Mevel K, Chetelat G, Eustache F, Desgranges B. The default mode network in  
704 healthy aging and Alzheimer's disease. *International journal of Alzheimer's disease*.  
705 2011;2011:535816.  
706 67. Sheline YI, Raichle ME. Resting state functional connectivity in preclinical  
707 Alzheimer's disease. *Biological Psychiatry*. 2013;74(5):340-7.  
708 68. Duval C, Daneault J-F, Hutchison WD, Sadikot AF. A brain network model  
709 explaining tremor in Parkinson's disease. *Neurobiology of Disease*. 2016;85:49-59.  
710 69. Müller-Oehring EM, Sullivan EV, Pfefferbaum A, Huang NC, Poston KL, Bronte-  
711 Stewart HM, et al. Task-rest modulation of basal ganglia connectivity in mild to  
712 moderate Parkinson's disease. *Brain imaging and behavior*. 2015;9(3):619-38.  
713 70. Owens-Walton C, Jakabek D, Li X, Wilkes FA, Walterfang M, Velakoulis D, et al.  
714 Striatal changes in Parkinson disease: An investigation of morphology, functional  
715 connectivity and their relationship to clinical symptoms. *Psychiatry Research: Neuroimaging*. 2018;275:5-13.  
716 71. Ponsen MM, Stam CJ, Bosboom JLW, Berendse HW, Hillebrand A. A three  
717 dimensional anatomical view of oscillatory resting-state activity and functional  
718 connectivity in Parkinson's disease related dementia: An MEG study using atlas-based  
719 beamforming. *Neuroimage: Clinical*. 2013;2:95-102.  
720 72. Guan X, Zeng Q, Guo T, Wang J, Xuan M, Gu Q, et al. Disrupted Functional  
721 Connectivity of Basal Ganglia across Tremor-Dominant and Akinetic/Rigid-  
722 Dominant Parkinson's Disease. *Front Aging Neurosci*. 2017;9:360.  
723 73. Eckert T, Tang C, Eidelberg D. Assessment of the progression of Parkinson's disease:  
724 a metabolic network approach. *The Lancet Neurology*. 2007;6(10):926-32.  
725 74. Szewczyk-Krolikowski K, Menke RA, Rolinski M, Duff E, Salimi-Khorshidi G,  
726 Filippini N, et al. Functional connectivity in the basal ganglia network differentiates  
727 PD patients from controls. *Neurology*. 2014;83(3):208-14.  
728  
729  
730  
731  
732  
733  
734

## 735 **Supporting Information captions**

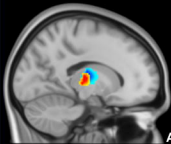
736  
737 **Supplementary Table S1. Correlations between functional connectivity and clinical data.** All  
738 values are rounded to two decimal places. VLp/VA thalamus, clusters 1-6, MD/A thalamus clusters 7-  
739 9. Significance based on a two-tailed Pearson correlation controlling for age, sex and years of  
740 education. A correction for multiple comparisons using the Bonferroni method stipulate a  $p$ -value of <  
741 0.000925 required for significance (based on performing 54 analyses). LED, levodopa equivalent  
742 dosage; UPDRS-III, Unified Parkinson's Disease Rating Scale part III; TUG, Timed Up and Go test;  
743 AQT, A quick test of cognitive speed test; AF, Animal fluency test.

744

745 **Supplementary Table S2. Correlations between thalami volumes and clinical measures: PD and**  
746 **Controls.** A correction for multiple comparisons using the Bonferroni method stipulate a  $p$ -value of <  
747 0.00625 required for significance (based on performing 8 analyses). UPDRS-III, Unified Parkinson's  
748 Disease Rating Scale part III; TUG, Timed up and Go test; AQT, A Quick Test of Cognitive Speed;  
749 AF, Animal Fluency test;  $R^2$  change, variance in clinical measure score explained by unique  
750 contribution of the volume of interest (multiply by 100 to find percentage);  $\beta$ , standardized beta  
751 coefficient, indicating effect size.

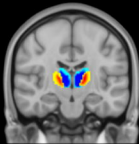
VLp/VA voxels  
MD/A voxels

Atlas-based seed-ROI placement



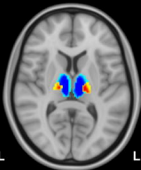
x = -15

A



y = -17

L



z = 8

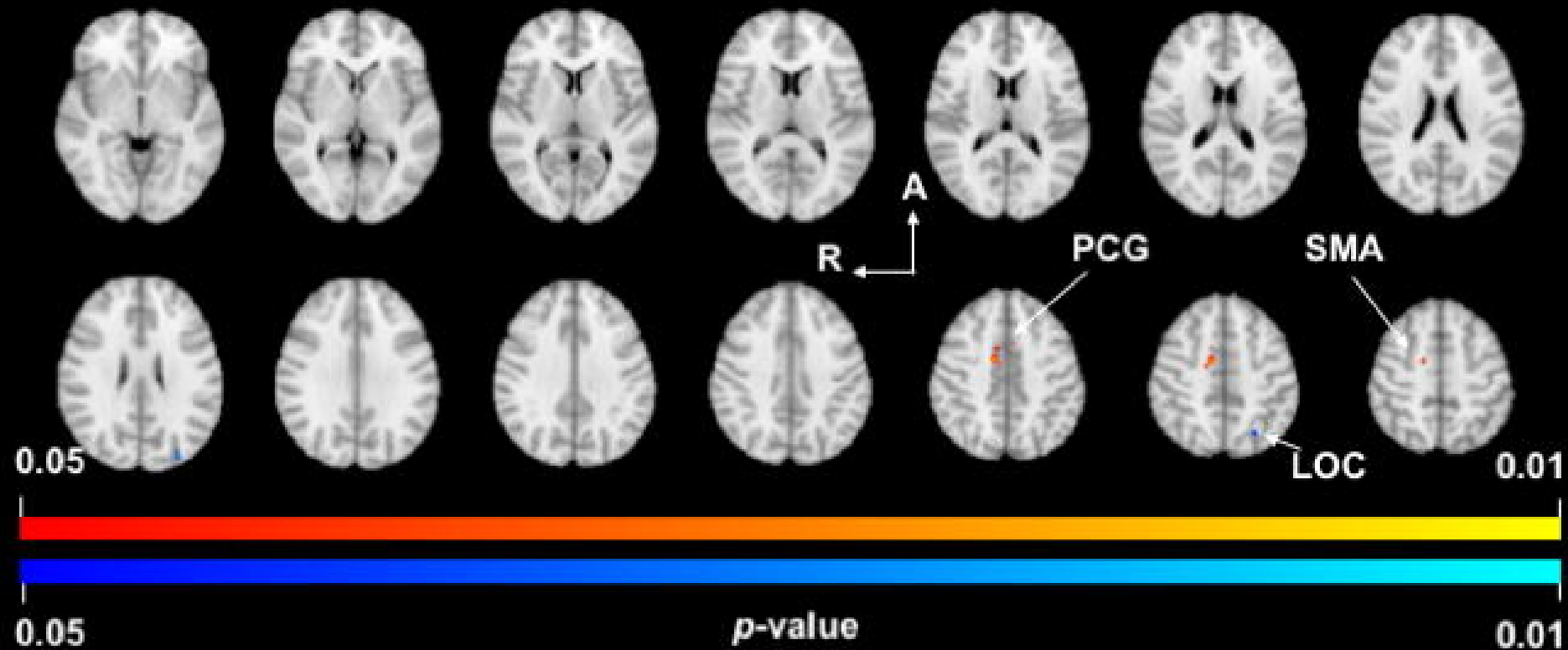
L

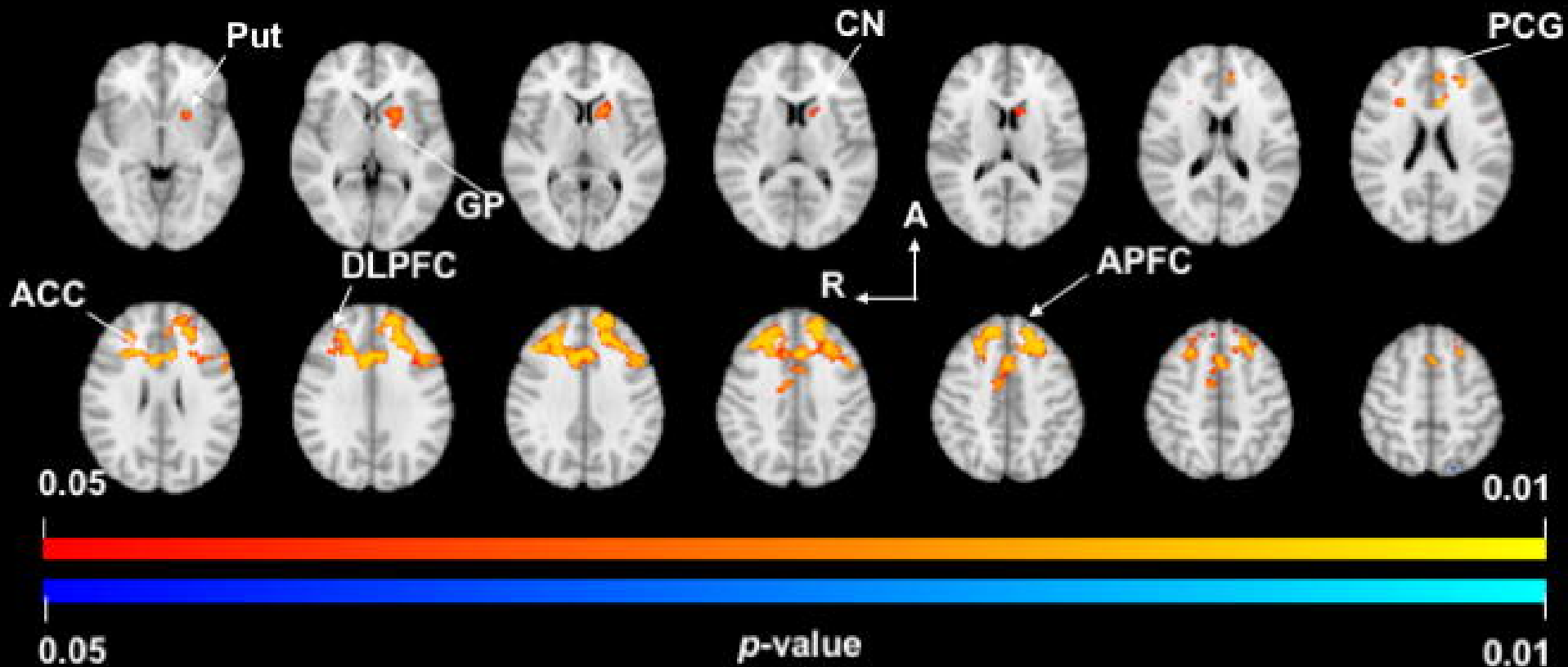
1%

50%

100%

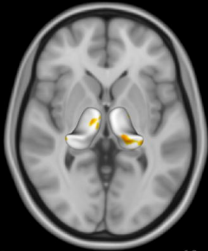
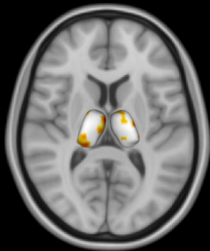






Superior

Inferior



0.0

0.25

0.5

Significant Displacement (mm)